

Gold nanorods-assembled ZnGa₂O₄:Cr nanofibers for LED-amplified gene silencing in cancer cells

Lun Qin,^a Peijian Yan,^b Congkun Xie,^a Jie Huang,^c Zhaohui Ren,^a Xiang Li,^{*a} Serena Best,^d Xiujun Cai,^b Gaorong Han^a

Received 00th January 20xx,
Accepted 00th January 20xx

DOI: 10.1039/x0xx00000x

www.rsc.org/

Nanoparticles are now commonly used as non-viral gene vectors for RNA interference (RNAi) in cancer therapy but suffer from low targeting efficiency in-situ. Meanwhile, localized drug delivery systems do not offer the effective capability for intracellular gene transportation. We describe here the design and synthesis of a localized therapeutic system, consisting of gold nanorods (Au NRs) loaded with hTERT siRNA assembled on the surface of ZnGa₂O₄:Cr (ZGOC) nanofibers. This composite system offers the potential for LED-induced mild photothermal effect which enhances phagocytosis of Au NRs carrying siRNA and the subsequent release of siRNA in cytoplasm. Both phenomena amplify the gene silencing effect and consequently offer the potential for a superior therapeutic outcome.

Introduction

RNA interference (RNAi) is one of the gene therapy approaches offered following tumor resection and has attracted interest in cancer treatment due to its high specificity and efficiency and the relatively minor side effects.¹⁻² Telomerase is highly expressed in almost all types of cancer cells but not in normal cells. The activity inhibition of telomerase using human telomerase reverse transcriptase (hTERT) has therefore been investigated in oncology.³⁻⁵ However, significant challenges remain in the efficient delivering delivery of hTERT siRNA at both at the tissue- and intracellular levels.⁶⁻⁸

In general, ideal non-viral gene vectors offer characteristics, such as chemical stability, biocompatibility, effective targeting, stimulus responsiveness and feasibility for combined treatments (i.e. chemotherapy, photothermal therapy, photodynamic therapy, etc.).⁹⁻¹² Gene delivery vectors reported in the recent years, include polymer-based, lipid-based, and inorganic nanoparticle-based systems.¹³⁻¹⁷ Surface-modified Au nanomaterials are recognized as promising gene delivery vehicles.¹⁸⁻²¹ Au nanoparticles (or nanorods) modified with cationic polymers (i.e. PEI, Chit, PDDAC, etc.) can be bound effectively to negatively surface charged siRNA molecules via a layer-by-layer approach. Due to their unique combination of surface plasmon properties and nanometer-scale dimensions,

effective intracellular delivery of Au nanoparticles can be achieved along with transfected siRNA in-vitro. However, the technique suffers from relatively low targeting efficiency in cancerous tissue during blood circulation.²²

Particulate systems can be associated with the circulation of excessively high concentrations of drugs in vivo. Localized Drug Delivery Systems (LDDSs) offer the potential to target the drug more effectively.²³ In recent years, a series of studies has shown that LDDSs can serve as successful therapeutic platforms and can inhibit a number of different types of cancer.²⁴⁻²⁵ Following injection of drug-loaded LDDSs at the tumor site, an external (or internal) stimulus is applied and the drug is released from the carrier in a controlled manner, to achieve 'on-site' chemotherapy.^{24, 26-28} However, for gene therapy in general, siRNA molecules are required to be phagocytosed and hence need to overcome extracellular and intracellular obstacles and be released from the endosome after being internalized by tumor cells.⁹ LDDSs, which are designed to manipulate the tumor microenvironment are normally injected (or implanted), have intrinsic drawbacks in achieving effective gene therapy. Therefore, by combining LDDSs and particulate gene carriers (i.e. gold nanorods) unique opportunities might be offered allowing controlled delivery and release of a targeted therapeutic concentration and effective phagocytosis of siRNA molecules for enhanced gene therapy.

Photo-responsive systems have also been investigated recently which allow spacio-temporal control of release kinetics for the delivery of therapeutic factors.²⁹⁻³⁰ Chromium-doped zinc gallate nanoparticles ZnGa_{2-x}O₄:Cr_x (ZGOC), under the excitation of a white LED (400-700 nm) light, can emit near-infrared spectra (650-750 nm) with high intensity and long afterglow lifetime.³¹⁻³² Unlike other contrast agents, no external light sources needed, auto-fluorescence and hence an enhanced signal-to-noise ratio can be achieved, thus offering a potential nontoxic optical probe for bioimaging purposes.³³⁻³⁵ Deep tissue

^a State Key Laboratory of Silicon Materials, School of Materials Science and Engineering, Zhejiang University, Hangzhou 310027, P. R. China.
Email: xiang.li@zju.edu.cn

^b Key Laboratory of Endoscopic Technique Research of Zhejiang Province, Sir Run Run Shaw Hospital, Zhejiang University, Hangzhou 310027, P. R. China

^c Department of Mechanical Engineering, University College London, Torrington Place, London WC1E 7JE

^d Department of Materials Science and Metallurgy, University of Cambridge, Cambridge CB3 0FS, UK

Electronic Supplementary Information (ESI) available. See DOI: 10.1039/x0xx00000x

imaging with a long period has been achieved *in vivo* using repeated excitation with low-energy LEDs.^{36–38}

In this work, we report a new type of localized gene delivery system with LED-responsive properties based on the combination of the LDDSs and nanoparticle gene vectors described above. In our system, hTERT siRNA was grafted on to Au NRs and these were attached to the surface of electrospun ZGOC nanofibers (Fig. 1). Au nanorods with an absorption peak of 700 nm matching the emission of ZGOC nanofibers were prepared using a seed growth method. Gold nanorods modified with a cationic polymer (PEI) were electrostatically bound with negatively charged siRNA. Under LED radiation, the ZGOC nanofibers emission could be absorbed selectively by Au NRs, inducing mild photothermal effect which in turn triggers the liberation of the particles from ZGOC nanofibers (LDDSs), and enhances the cell up-taking and the therapy effect. The new therapeutic platform, with LED-amplified gene silencing has therefore inspired another potential system for enhance gene therapy in cancer treatment.

Results and discussion

ZGOC nanofibers with photoluminescence

Following electrospinning and sintering at 800 °C, SEM and TEM images confirmed that the ZGOC nanofibers had a roughened surface at the nanoscale, but a relatively uniform microstructure and uniform diameters of the order of 100 nm (Fig. 2a & 2b). The fibres comprised an assembly of fine crystals, and the embedded HRTEM lattice image reveals that a d-spacing of 0.249 nm, which can be attributed to (311) planes of ZnGa₂O₄ crystal (PDF # 38-1024) (Fig. 2b). The XRD trace had sharp diffraction peaks attributable to the cubic-phase of highly crystalline ZnGa₂O₄ and the absence of extraneous peaks confirmed the phase purity of the prepared ZGOC nanofibers (Fig. 2c). The EDS analysis showed that the fibres comprised a homogeneous distribution of Zn, Ga, O and Cr (Fig. S2a). The fibres exhibited a broad excitation spectrum ranging from UV to the visible band (~350 to 600 nm, Fig. S2b) when exposed to a Xenon lamp (FLSP920, Edinburgh Instruments) and emitted a strong near-infrared broad-band emission (600 ~ 800 nm) along with two sharp

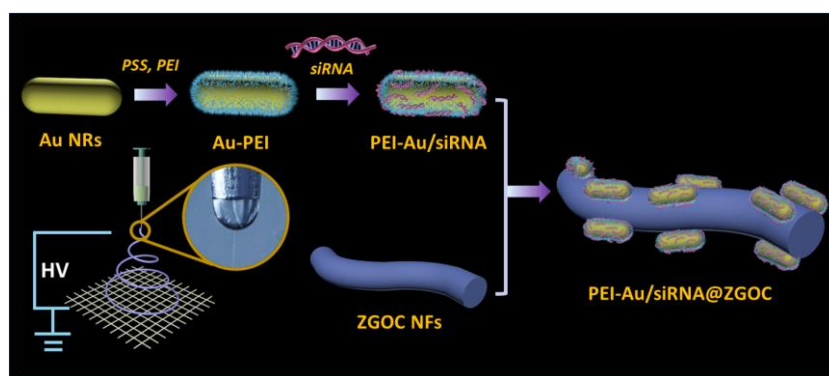


Fig. 1 Schematic illustration of the fabrication of PEI-Au/siRNA@ZGOC composite.

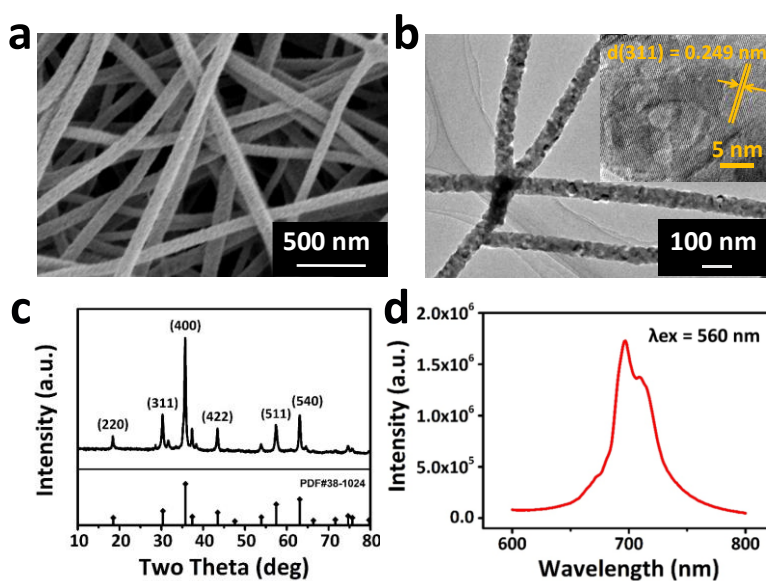


Fig. 2 Characterization of ZnGa₂O₄: 0.5 % Cr³⁺ nanofibers (ZGOC nanofibers). (a) SEM image of ZGOC nanofibers. (b) TEM image of a ZGOC nanofibers, Inset: High-magnification. (c) X-ray diffraction pattern of ZGOC nanofibers with 0.5 mol % Cr³⁺ doped. (d) PL emission spectrum of ZGOC nanofibers, under Xenon lamp excitation at 560 nm.

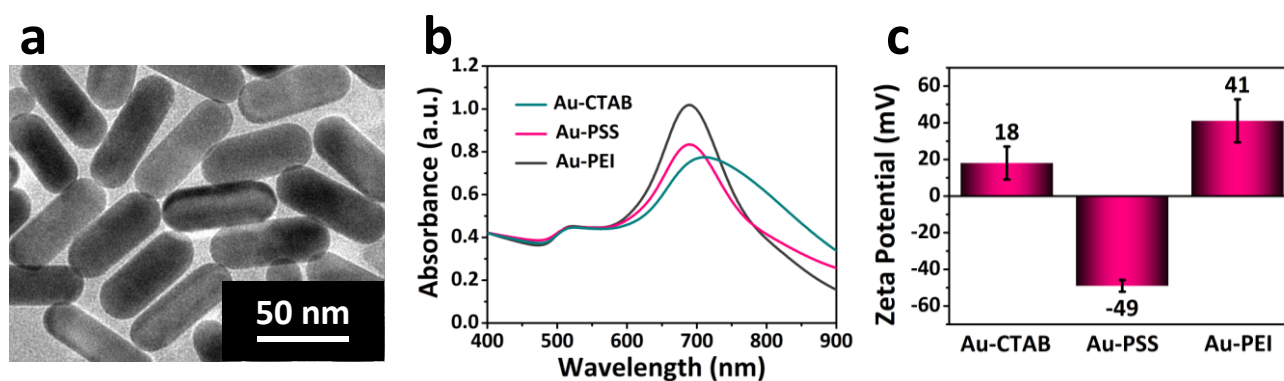


Fig. 3 Characterization of PEI-Au NRs. (a) Transmission electron microscopy (TEM) images of PEI-Au NRs. (b) Ultraviolet visible (UV-Vis) spectra of Au-CTAB, Au-PSS, Au-PEI NRs in aqueous solution. (c) Zeta potential of Au-CTAB, Au-PSS, Au-PEI NRs in aqueous solution. Results are presented as the mean of five measurements \pm standard deviation.

peaks (~ 700 nm and ~ 710 nm) when excited at 560 nm (Fig. 2d). The broad emission band was assigned to the spin-allowed transition of Cr^{3+} (${}^4\text{T}_2 \rightarrow {}^4\text{A}_2$), while the narrow-band emission was attributed to spin-forbidden transition of Cr^{3+} (${}^2\text{E} \rightarrow {}^4\text{A}_2$).^{33,36,39} It is also noted that the as-prepared ZGOC fibres present a luminescence decay time of only a few seconds (Fig. S2c). Liquid phase reaction, such as sol-gel electrospinning, is feasible for synthesizing fine fibres with lower dimensions, uniformity and controllable morphology, but meanwhile it may lead to reduced luminescence decay time of nanofibers due to less point defects induced in the crystal structure.⁴⁰

PEI-modification of Au NRs

A high intensity emission peak occurred for ZGOC fibres at ~ 700 nm. To ensure that the fibres emission could be absorbed effectively by grafted Au NRs structures, samples with different surface plasmon resonance bands were prepared (Fig. S3). When 900 μL of 10 mM AgNO_3 solution was added, the resulting Au NRs demonstrated adsorption at ~ 700 nm. The particles had a uniform morphology, with lengths and widths of ~ 70 nm and ~ 30 nm, respectively (hence an aspect ratio of 2.3, Fig. 3a).⁴¹ Polyethyleneimine (PEI) is a well-known non-viral nucleic acid vector with high transfection efficiency both in vitro and in vivo due to the high density of positively charged amino groups distributed along the backbones of the molecular chains.⁴³ The surfaces of the as-prepared Au NRs produced via the seed-mediated growth method were covered by a layer of CTAB molecules with positive charge. Prior to the PEI modification, a PSS layer was initially formed at the particle surface by electrostatic adsorption to obtain the negatively charged PSS-modified Au NRs (Au-PSS). The as-prepared Au NRs (Au-CTAB) exhibited a weak transverse surface plasmon resonance (TSPR) band at ~ 520 nm and a strong longitudinal surface plasmon resonance (LSPR) band at ~ 700 nm (Fig. 3b). After coating with PEI, the absorbance of the Au-PEI samples showed a red shift of ~ 20 nm. This is due to the increased local refractive index of the surrounding medium after replacing CTAB with the PSS and PEI layers.^{43,44} The maximum absorption of Au NRs reached ~ 700 nm after PEI-modification, which matches well with the emission spectrum of the ZGOC fibres. The Zeta potential values of Au-CTAB, Au-PSS and Au-PEI were $\sim +18$ and ~ -49 and $\sim +41$ mV, respectively (Fig. 3c). The results demonstrated clearly the

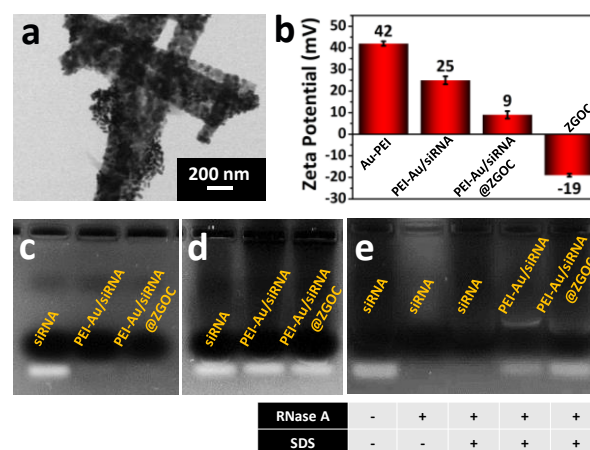


Fig. 4 (a) TEM image of PEI-Au/siRNA@ZGOC nanocomposites. (b) Zeta potential value of several substances. Results are presented as the mean of five measurements \pm standard deviation (c) agarose gel retardation assay of PEI-Au/siRNA and PEI-Au/siRNA@ZGOC complexes. Naked siRNA was used as a control. (d) Profile of siRNA release from PEI-Au/siRNA and PEI-Au/siRNA@ZGOC complexes. (e) Protection of siRNA against RNaseA digestion and siRNA release by competitive binding sodium dodecyl sulfate (SDS) with carriers after degradation. Naked siRNA was used as a control. (PEI-Au/siRNA complexes were prepared at a weight ratio of 25:1, while PEI-Au/siRNA@ZGOC complexes were 25:25:1)

positive surface charge of Au-PEI NRs and their ability to deliver siRNA.

Construction of PEI-Au/siRNA@ZGOC gene carriers

The positively-charged Au-PEI NRs possess the ability to electrostatically bind to negatively-charged siRNA. The optimal binding ratio of Au-PEI NRs to siRNA was investigated using an agarose gel electrophoresis assay and by measuring Zeta potential (Fig. S4). Based on the results obtained in Fig. S4a, a PEI-Au/siRNA mass ratio of 25:1 was selected for further study. Following the self-

assembly procedure, TEM images of PEI-Au/siRNA@ZGOC nanocomposites indicated good cohesion between the particles and the fibres (Fig. 4a). The Zeta potential of Au-PEI, PEI-Au/siRNA, PEI-Au/siRNA@ZGOC and ZGOC samples were $\sim+42$, $\sim+25$, $\sim+9$ and ~-19 mV respectively, in aqueous solution (Fig. 4b). The PEI-Au/siRNA@ZGOC complex showed a weak positive charge, which would be likely to complement well the negative charge of the surface membrane of cancer cells. The binding affinity of PEI-Au/siRNA and PEI-Au/siRNA@ZGOC samples was initially compared using agarose gel electrophoresis. As shown in Fig. 4c, siRNA molecules were successfully bound to both vectors resulting in the disappearance of the siRNA band, whereas the free siRNA, without the vector, showed a bright band of siRNA. When treated with SDS, the electrostatic interactions between the siRNA and the carriers were destroyed, and thus siRNA was released, leading to the re-appearance of siRNA bands at a similar level (Fig. 4d). This reflects the potential for siRNA release into the cytoplasm, via the breakdown of the electrostatic interactions within the carrier. In addition, comparing to gene therapy based on particle-form vectors, the serum stability of localized gene delivery systems, which do not require sufficient system circulation, mainly depends on the protection of gene from degradation by DNase or RNase by the carriers. The protection of siRNA by PEI-Au/siRNA and PEI-Au/siRNA@ZGOC vectors was further verified by the addition of RNaseA to mimic the human serum environment. The PEI-Au/siRNA and PEI-Au/siRNA@ZGOC vectors were found to protect the siRNA, effectively, from the degradation effects of RNaseA (Fig. 4e). When free siRNA, PEI-Au/siRNA and PEI-Au/siRNA@ZGOC were treated with RNaseA followed by SDS treatment, siRNA without carrier-

protection was found to be decomposed by RNaseA and the siRNA band disappeared from the agarose. In contrast, with the protection of the two vectors, the RNA bands were clearly visible in the agarose gel. Therefore, we have constructed a LDDS gene vector system of PEI-Au/siRNA@ZGOC which binds siRNA. The assemblies protected siRNA in an RNase environment and released siRNA by breaking electrostatic interactions - a key factor for their successful application as a gene delivery system.^{18,19}

Mild photothermia effect triggered by cold LED light

Before exploring the photothermal properties of the complex, an investigation was undertaken, of the influence of mass ratio between PEI-Au/siRNA particles and ZGOC nanofibres on the photoluminescence of PEI-Au/siRNA@ZGOC fibres. The corresponding photoluminescence emission spectra were obtained using xenon lamp excitation (~ 560 nm). As shown in Fig. 5a, the emission at ~ 700 nm from the ZGOC nanofibres is gradually absorbed by Au-PEI with increasing mass ratio, resulting in a decline in intensity. At a mass ratio of 1:1, no luminescence was detected, indicating that all emission of ZGOC fibres is absorbed by PEI-Au/siRNA particles, and this particle/fibre mass ratio was used for further in vitro studies. Under irradiation by a white LED light with a power density of 0.18 W/cm², the temperature of PEI-Au/siRNA@ZGOC solution increases, and pure water present marginal photothermal effect ($\Delta T < 1$ °C). Prolonged irradiation and increased concentration induced more marked heating effects, as demonstrated by the results from the infrared thermophotometry camera. After 5 min of LED irradiation, the solution temperature rose by 5 °C when the concentration of PEI-Au/siRNA@ZGOC was set at 50 $\mu\text{g}/\text{mL}$ (Fig. 5b & 5c).

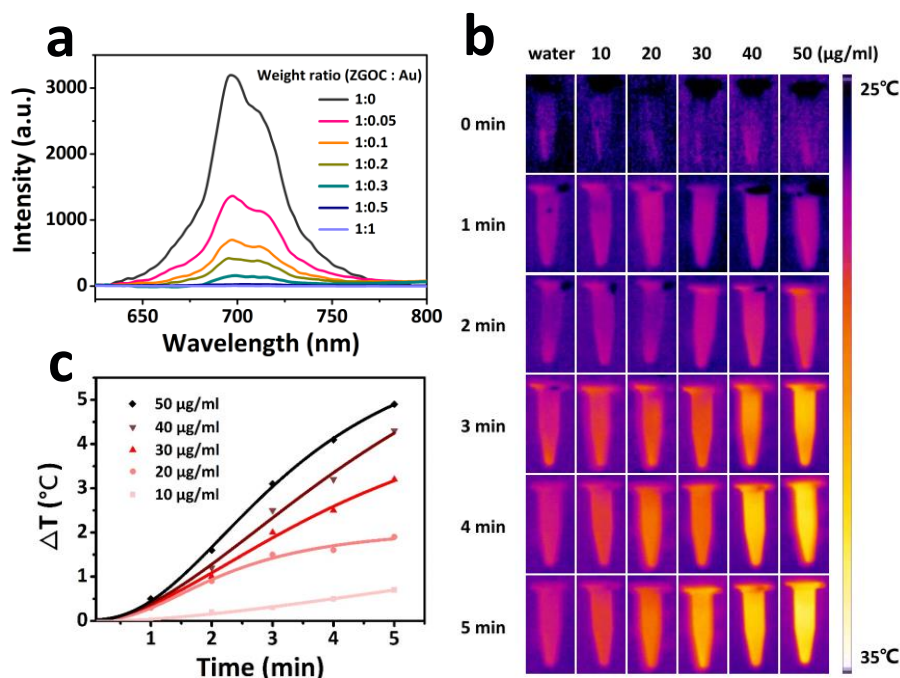


Fig. 5 Optimization of PEI-Au/siRNA@ZGOC systems. (a) PL emission spectrum of PEI-Au/siRNA@ZGOC composites of different weight ratios, under Xenon lamp excitation at 560 nm. (b), (c) Temperature variation curves and temperature images of PEI-Au/siRNA@ZGOC composites in different concentrations under LED irradiation for minutes. The white LED light has a power density of 0.18 W/cm².

Compared with the individual therapeutic approaches, this mild photothermal synergistic gene therapy strategy shows promising characteristics for cancer treatment. The mild photothermal effect (≤ 43 °C) may result enhanced benefits by overcoming the various barriers to intracellular gene delivery (such as cellular uptake, endosome escape, and cytosolic gene release).⁴⁵ In this work, the gold nanorods synthesized exhibited an absorption band at ~ 700 nm, which overlaps the emission of the ZGOC fibres. This unique design enables an effective transfer from 'cold' LED light to a mild heating phenomenon. While systems responsive to NIR light (700-1000 nm) have achieved considerable success, they suffer considerable concerns in tissue due to the damage caused by the uncontrolled thermal effects of NIR absorption.⁴⁶ In this respect, the use of white LED light (400-700 nm), which induces a low-level and entirely tolerable heating effect, offers unique advantages in suppressing side effects during therapeutic treatment.

Au-PEI release property from ZGOC nanofibers by cold LED light

PEI-Au/siRNA@ZGOC complexes immersed in deionized water were exposed under LED light for 5 minutes, and the microstructure of composite fibres before and after LED irradiation was examined using transmission electron microscopy. As expected, the gold nanorods (Au-PEI) remain assembled at the surface of as-prepared ZGOC nanofibers by electrostatic adsorption after immersion in water (Fig. 6a). After the LED irradiation for 5 minutes, the majority of gold nanorods liberate from ZGOC fibres (Fig. 6b). In consequence, the PL intensity of the composite fibres increases remarkably with

the releasing progress of Au NRs induced by LED irradiation. (Fig. 6c). Under the LED irradiation, the emission of ZGOC fibres is effectively absorbed by Au NRs assembled at the surface, enabling the mild heating effect at the particle/fibre interface. As a result, the electrostatic bonding between ZGOC fibre and Au NRs is weakened due to thermal vibration, inducing the characteristic of LED-responsive PEI-Au/siRNA release from the system.

In vitro cyto-compatibility and anticancer study

For the clinical implementation of therapeutic systems, it is crucial to consider the biocompatibility and safety of the materials involved. The cytotoxicity of PEI-Au and PEI-Au@ZGOC complexes (without siRNA) was examined using HepG2 cells and an MTT assay. Cells were incubated with the samples for 24, 48 and 72 h and the cell viability remained at over 85 % at a concentration of 0-100 $\mu\text{g}/\text{mL}$, reflecting that neither of the two vectors impacted negatively on cyto-compatibility (Fig. 7a & 7b). In general, the PEI with 25 kDa is toxicity to the normal and tumour cells when the high doses are involved.⁴⁷ The cells showed relatively high survival rate (above ~ 85 %) when the concentration of PEI was below 8 $\mu\text{g}/\text{mL}$ (Fig.S5). It is worth noting that, in our study, the PEI 25 kDa was used as a means of surface modification of Au NRs, rather than the substrate carriers for genes. Although the concentration of PEI modified Au NRs used in this study is 50 $\mu\text{g}/\text{mL}$, Au, which is a heavy metal element, occupies most of its mass. The cyto-compatibility of our system is attributed to the low content of PEI molecules grafted at the surface of Au NRs. A variety of studies have reported the similar phenomenon that grafting PEI

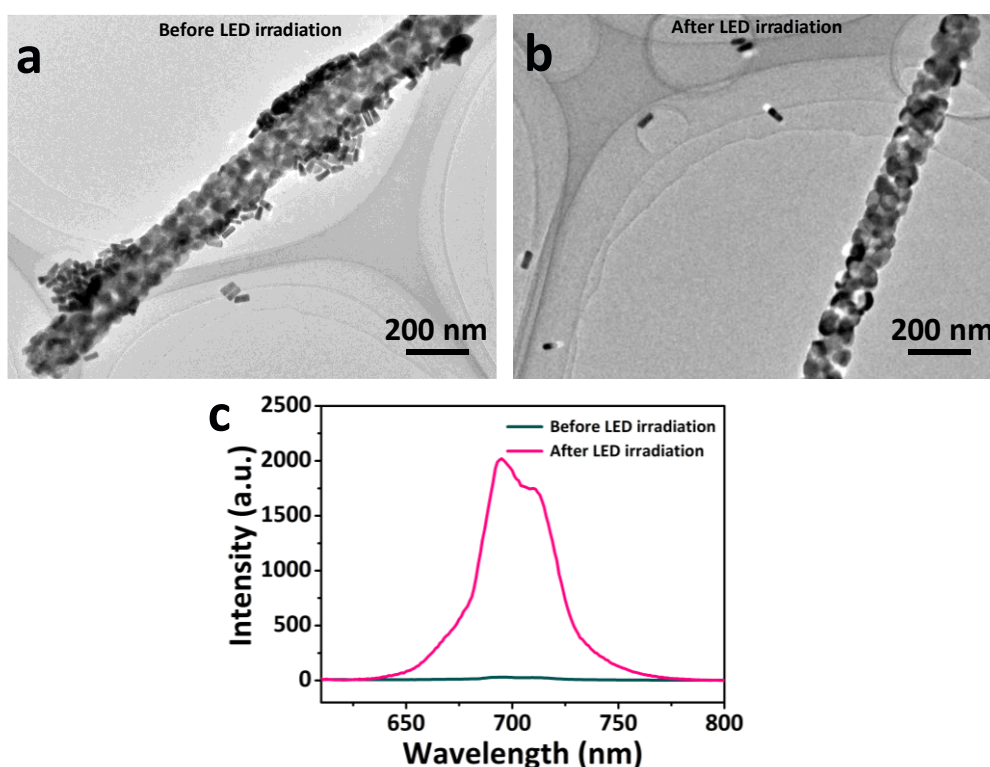


Fig. 6 TEM images of PEI-Au/siRNA@ZGOC composite fibres (a) before and (b) after the LED ($0.18 \text{ W}/\text{cm}^2$) illumination of 5 min.; (c) The PL intensity of the composite fibres before and after LED excitation.

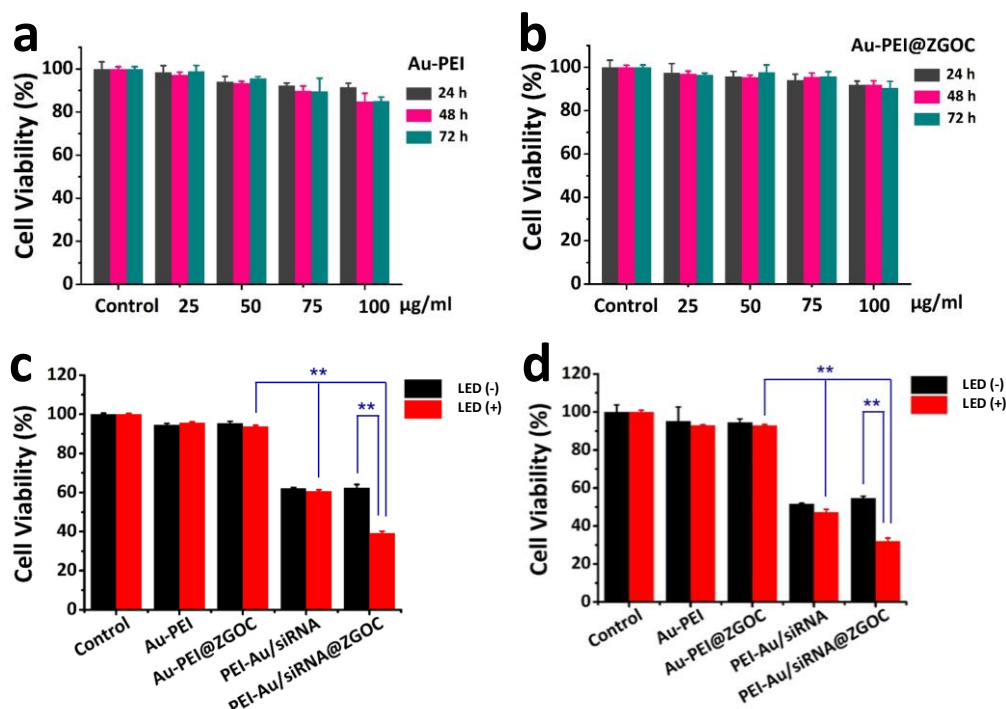


Fig. 7 MTT assay of cell viability following incubation with PEI-Au NRs (a) and PEI-Au@ZGOC, (b) for 24, 48, 72 h; (c)(d) Cell viability incubation with PEI-Au/siRNA and PEI-Au/siRNA@ZGOC in response to LED for 48 h and 72 h. Results are presented as the mean of three measurements \pm standard deviation.

(25 kDa) molecules with delivery systems, as a means of surface modification, does not induce clear cytotoxicity.^{48,49}

The anti-cancer effects of the PEI-Au/siRNA and PEI-Au/siRNA@ZGOC samples were assessed via in-vitro cell culture for 48 h and 72 h, using exposure to LED light. Untreated cells were used as a blank control and the siRNA concentration was set at 100 nM for all samples. As shown in Fig. 7c and 7d, cell proliferation in the sample groups loaded with siRNA was significantly inhibited (by over 40%). LED radiation did not appear to induce any clear effect on the PEI-Au/siRNA group but, in contrast the PEI-Au/siRNA@ZGOC group showed a significant decrease in cell viability under LED irradiation.

Gene silencing effect

mRNA and protein expression level analysis

The key to the success of RNAi lies in the effect release of siRNA from the endosome, so that it can destroy the target mRNA in the cytoplasm to inhibit the expression of the target protein. The hTERT mRNA level and the hTERT protein expression level in the cells were evaluated by RT-PCR and Western blotting. Studies have shown that the expression level of hTERT is related to the proliferation of HepG2 cancer cells.^{5, 50} The results showed that hTERT siRNA transfection was able to inhibit hTERT expression both in mRNA and protein level (Fig. 8a & 8b). After 48 h of cell culture with different complexes, the expression of hTERT mRNA in cancer cells was significantly inhibited, and the inhibitory efficiency reached \sim 40% for the samples loaded with siRNA. When irradiated with LED light, the inhibition rate of PEI-Au/siRNA@ZGOC vector further decreased to 65%, while PEI-Au/siRNA sample remained unchanged, as expected (Fig. 8a). The

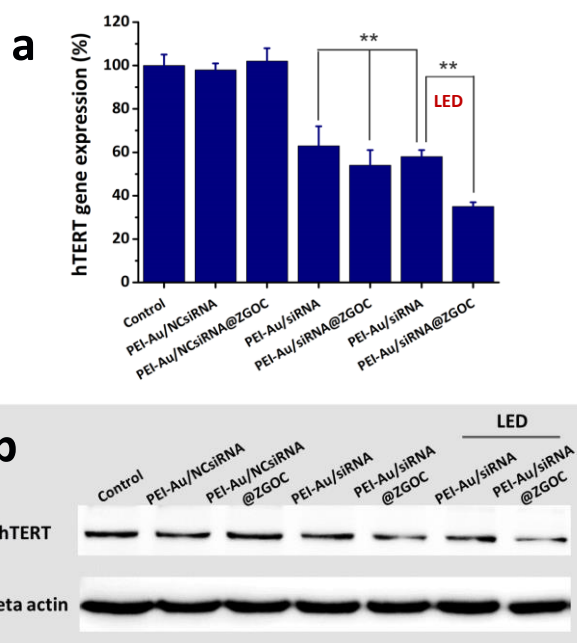


Fig. 8 Gene silencing effect of hTERT siRNA in HepG2 liver cancer cells. (a) qPCR analysis was used to evaluate mRNA levels. Cells were harvested 48 h later, and mRNA levels were measured by qPCR and normalized to GAPDH. Results are presented in the mean of three measurements \pm standard deviation. (b) Western blot analysis hTERT protein expression in HepG2 cells. beta-actin was used as an internal control. Cells were treated with 100 nM siRNA.

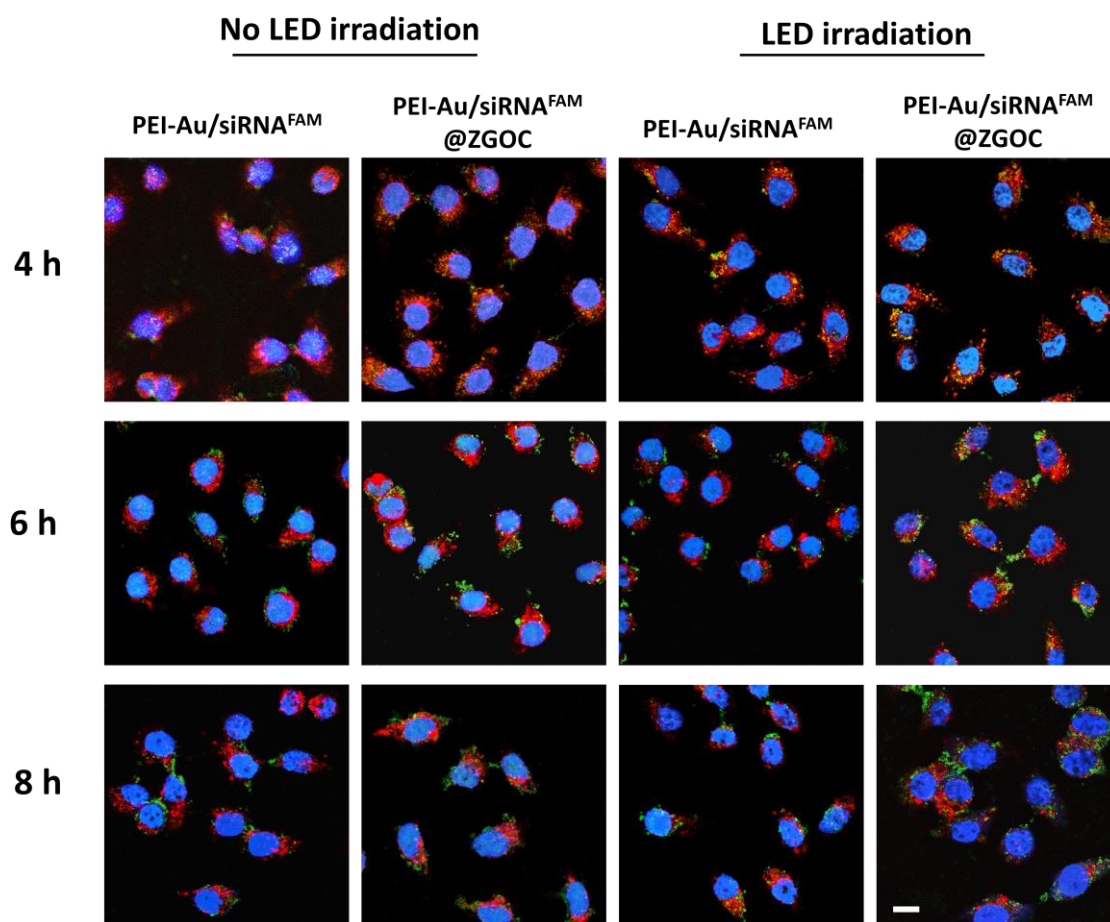


Fig. 9 Intracellular trafficking of PEI-Au/siRNA^{FAM} and PEI-Au/siRNA^{FAM}@ZGOC complexes in cell. Cells were harvested at the indicated time points and stained with LysoTracker Red for imaging endosome/lysosome structures (red) and DAPI for imaging the nuclei (blue). Fluorescent images were captured with a confocal microscope. The scale bar is 20 μ m.

results are in good agreement with the previous in vitro anti-cancer study. Similarly, Western blot analysis of hTERT protein expression after 72 hours incubation shares the same pattern (Fig. 8b).

Delivery of hTERT siRNA by PEI-Au/siRNA@ZGOC markedly reduced hTERT protein expression and after LED irradiation, the expression of hTERT protein level was suppressed more significantly. In contrast, control and NCsiRNA groups did not down-regulate hTERT protein expression in HepG2 cells, reflecting that no specific gene silencing occurred. The expression of hTERT protein extracted from cancer cells cultured for 72 h was consistent with the mRNA in vitro experiment. The difference between the vector groups and the control groups were statistically significant ($p < 0.01$).

Mechanisms

The findings demonstrate that the PEI-Au/siRNA@ZGOC group irradiated with LED shows enhanced protein inhibitory effects when compared to those tested without LED exposure. To study the effect of LED illumination on siRNA transfection, the intracellular transportation of FAM-siRNA (green) after culturing with both vectors (PEI-Au/siRNA and PEI-Au/siRNA@ZGOC) for several hours were examined by confocal microscopy (Fig. 9). After 4 hours of cell incubation, FAM-siRNA (green) co-localized with the

endosome/lysosome (red) with the result that almost all the FAM-siRNA located in endosomes/lysosomes to merge in orange outside the nucleus. The nanoparticles entered the cells to form endosome, while the ZGOC nanofibers with over-sized length cannot be taken up by cells. Owing to the negative potential of cell membrane, nanoparticles with positive surface charge can also induce phagocytosis efficiency by electrostatic interactions. The first three groups present a certain degree of green fluorescence, as expected. It is worth noting that the last sample group, which induces thermal effect under LED irradiation, presents strongest fluorescence (green) emission intensity than the others, implying that the heating promotes cellular internalization of the particles released. After 6 hours incubation, some siRNAs were present in the cytoplasm, accompanying the reproduction of green fluorescence, indicating that siRNA molecules had escaped from acidic endosomes/lysosomes. A closer examination revealed that the PEI-Au/siRNA@ZGOC with LED radiation had a stronger green fluorescence compared to the other groups, indicating higher efficiency of siRNA release after the LED radiation. The first three groups present a separated green fluorescence in the cytoplasm, attributing to the proton sponge mechanism of PEI, resulting in disrupting endosomal compartments and facilitating the releasing of

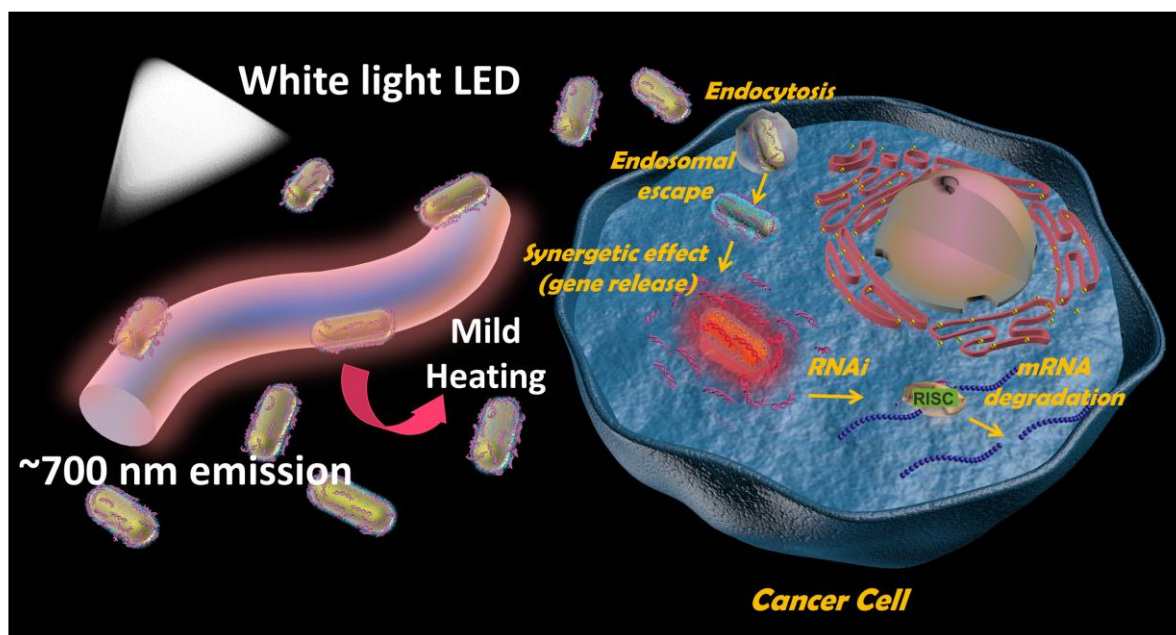


Fig. 10 Schematic illustration of the design of PEI-Au/siRNA@ZGOC nanofibers in the improved gene therapy platform

therapeutics from endosomes.⁵¹ For the last group, in addition to the PEI effect, the endosomal escape of siRNA from the lysosomes is enhanced by the promoted proton sponge effect owing to the LED-induced heating effect, enabling the improved transfection efficiency of siRNA. There was no significant difference between the 8-hour cell culture and the 6 hours experiment, indicating that endocytosis and endosome release of siRNA was completed after 6-hour culture.

A nano-scale platform for the delivery of therapeutic siRNA into solid tumors needs to overcome both extracellular and intracellular barriers. Once siRNAs are ingested inside tumor cells, they need to escape from the endosome into the cytoplasm, and finally release the siRNA payload to form RNA-induced silencing complex (RISC).⁹ The confocal images visually demonstrate that PEI-Au/siRNA and PEI-Au/siRNA@ZGOC have the ability to deliver siRNA to the interior of the tumor cells and achieve endosome escape of the siRNA. It is worth noting that the fibre-based LDDS delivery system has higher gene transfection efficiency.

Overall, the main mechanism of LED-illuminated fibre-based LDDS gene delivery system to improve the RNAi efficacy is as shown in Fig. 10. Here, the gold nanorods, acting as a photothermal energy converter, convert emission light from ZGOC fibres into heat, leading to an increase in the local temperature. The locally generated mild heating plays two roles: (1) promoting the release of gold nanorods from fibres extracellularly; (2) facilitating siRNA release in cytoplasm to form RISC. These two aspects enhance the therapeutic effect of gene silencing.

Conclusion

A localized therapeutic system, based on Au NRs and ZGOC nanofibers, has been designed and constructed for cancer gene

therapy. In this system, hTERT siRNA grafted Au NRs were assembled on the surface of electrospun ZGOC nanofibers. Au NRs have an absorption peak of 700 nm which matches the emission of ZGOC nanofibers under excitation of LED light. This composite system, PEI-Au/siRNA@ZGOC fibres, promotes the siRNA concentration in-situ. Under LED irradiation, a mild photothermal effect is induced that significantly facilitates the escape of siRNA from endosomes and improves the siRNA transfection efficiency. Consequently, the efficiency of gene silencing was markedly enhanced from ~40 % to ~65 %. Both phenomena enable superior in vitro anti-cancer effect. It is anticipated that this new therapeutic platform, based on LED-amplified gene silencing, will lead to a potential new generation of enhanced gene therapy treatments for a range of cancers.

Experimental Section

Materials and reagents

Zinc nitrate hexahydrate ($\text{Zn}(\text{NO}_3)_2 \cdot 6\text{H}_2\text{O}$, 99.95%), gallium nitrate hydrate ($\text{Ga}(\text{NO}_3)_3 \cdot x\text{H}_2\text{O}$, 99.99%) and chromium (III) nitrate nonahydrate ($\text{Cr}(\text{NO}_3)_3 \cdot 9\text{H}_2\text{O}$, 99%) were purchased from Macklin, China. Poly(vinylpyrrolidone) (PVP, Mw = 1,300,000), poly(sodium 4 styrenesulfonate) (PSS, MW=70,000) and branched Poly(ethyleneimine) (PEI, MW = 25 kDa) were supplied by Sigma-Aldrich. Sodium borohydride (NaBH_4), silver nitrate (AgNO_3), and L-ascorbic acid (AA) were purchased from Sinopharm Chemical, China. beta-actin and hTERT antibodies were purchased from Sangon biotech. GoldView™ was supplied by SBS genetech Co., Ltd. siRNA samples were synthesized by GenePharma Company, Shanghai, China (Table 1). All other reagents were obtained from Beyotime® Biotechnology. A purpose-designed LED light source was

Code	Sense sequence
NC siRNA	5' - GGC CUC AGC UGC GCG ACG CTT - 3'
NC siRNA ^{FAM}	5' - GGC CUC AGC UGC GCG ACG CTT - 3'
hTERT siRNA	5' - GAG CCA GUC UCA CCU UCA ATT - 3'
primer for hTERT	5' - TCA CGG AGA CCA CGT TTC AAA - 3' 3' - TTC AAG TGC TGT CTG ATT CCA AT - 5'
primer for GAPDH	5' - ACC CAC TCC TCC ACC TTT G - 3' 3' - CTG TAG CCA AAT TCG TTG TCA T - 5'

Table 1. siRNA sequences and the primer sequences of hTERT and GAPDH mRNA for qPCR amplification.

manufactured for in-vitro studies with the CoBs supplied by Philips Lumileds (Fig. S1).

Synthesis of ZGOC Nanofibers

The synthesis of ZGOC nanofibers was performed using via the modified a modified protocol based on previous studies reported in the literature.⁵²⁻⁵⁴ The electrospinning precursor was prepared by a standard sol-gel approach. Ga(NO₃)₃·xH₂O (0.475 g), Zn(NO₃)₂·6H₂O (0.279 g) and Cr(NO₃)₃·9H₂O (0.002 g) were added to 2 mL deionized water 6 mL ethanol and 3 mL N,N-dimethylformamide (DMF) and mixed well by stirring for 1 h. Subsequently, 0.7 g PVP was added and stirred for further 3 h to obtain a homogeneous solution. ZGOC nanofibers were electrospayed using a flow rate of 0.18 mL/h, controlled by a propulsion pump. A high-voltage electric field of ~9 kV was applied between the needle tip and an earthed steel mesh where the fibres were collected. A stable cone-jet was maintained throughout the synthesis process and observed by a high-speed camera (Baumer, TXG04h, Germany). The fibres were collected and sintered in a muffle furnace at 800 °C for 6 h.

Synthesis of Au NRs and Surface Modification

Gold nanorods (Au NRs) were prepared according to a seed-mediated growth method.⁵⁵⁻⁵⁶ For the seed solution, an aqueous CTAB solution (5 mL, 0.2 M) was mixed, using vigorous stirring, with HAuCl₄ (5 mL, 0.5 mM) and ice-cold NaBH₄ (1 mL, 6 mM). After placing the mixture in a 25 °C water bath for 30 min, a brownish-yellow seed solution resulted. To prepare the growth solution, CTAB (100 mL, 0.1 M) was mixed with AgNO₃ (10 mM), followed by the addition of HAuCl₄ (100 mL, 1 mM). The volume of silver nitrate solution added was varied from 600-1000 µL, to produce Au NRs with different absorption peaks. Ascorbic acid (1.6 mL, 0.1 M) was then added and the solution was stirred vigorously for 30 s until it became colorless. Finally, 240 µL of a gold seed solution was injected into the stirred growth solution and aged for 12 h at 30 °C. The precipitate was centrifuged (8000 rpm for 20 min) and re-dispersed in pure water. PEI-Au NRs with positive charge were obtained via a layer-by-layer assembly approach.¹⁹ The negatively charged Au NRs were obtained by first assembling a PSS layer on the original Au NRs. Briefly, 10 mL as prepared Au NRs (Au-CTAB) was centrifuged at 8000 rpm for 20 min, and the precipitate was dispersed in 10 mL of PSS aqueous solution (2 mg/mL). After being stirred for 3 h at 30 °C, the

sample obtained was dispersed in an equal volume of PEI solution (2 mg/mL). PEI-Au NRs were collected through several rounds of centrifugation, followed by re-suspension in nuclease-free water (DEPC water) and stored at 4 °C for further use.

Optimization of PEI-Au/siRNA systems.

siRNA solutions (0.02 µg, 10 µL) were combined with PEI-Au NRs (10 µL) at various weight ratio (PEI-Au/siRNA = 5:1, 10:1, 15:1, 20:1, 25:1 and 30:1), respectively. The resulting solutions were combined with a vortex mixer for 1 min and then incubated at 4 °C for 30 min. The binding of siRNA to PEI-Au NRs was confirmed using 1 % agarose gel electrophoresis (25 mL) containing 2.5 µL GoldViewTM. Electrophoresis was carried out at a constant voltage of 120 V for 20 min in TAE running buffer. siRNA bands were examined in a UV transilluminator was used to visualize the siRNA bands. The concentration of Au NRs in the solution was examined by inductively coupled plasma mass spectrometry (ICPMS).

Preparation of PEI-Au/siRNA@ZGOC

Composite Nanofibers. The Au-PEI particles and ZGOC nanofibers, which have opposite surface charge, were combined by self-assembly. Weight ratios of 1: 0, 1: 0.05, 1: 0.1, 1: 0.2, 1: 0.3, 1: 0.5 and 1: 1 Au-PEI/siRNA (1.5 mL, 1 mg/mL): ZGOC fibres suspension were shaken gently (100 rpm) overnight at 30 °C. Free Au-PEI NRs were washed away using centrifugation (4000 rpm, 10 min). The resulting complexes were re-suspended in deionized water. To determine the optimal proportion of Au NRs and ZGOC fibres, the PL spectra were recorded of the PEI-Au/siRNA@ZGOC fibres excited using a xenon lamp from a fluorescence spectrophotometer (FLSP920, Edinburgh). The photothermal effect of PEI-Au/siRNA@ZGOC solutions with different concentrations (0, 10, 20, 30,40 and 50 mg/mL) were estimated under the excitation by white LED light at a power density of 0.18 W/cm² for up to 5 min at room temperature. An infrared thermal imaging instrument (FLIR, E40, USA) was used to monitor the changes in temperature.

Au-PEI release property from ZGOC nanofibers by cold LED light

The PEI-Au/siRNA@ZGOC composite (weight ratio=1:1) was selected and immersed in deionized water. After the LED irradiation at a power density of 0.18 W/cm² for 5 min, the samples before and after the LED illumination were centrifuged at 4000 rpm for 10 min, and examined via TEM. The photoluminescence emission intensity spectra of two samples were recorded using a xenon light (560nm excitation) from a fluorescence spectrophotometer (FLSP920, Edinburgh).

siRNA Release Kinetics of PEI-Au/siRNA and PEI-Au/siRNA@ZGOC systems

siRNA release from two vehicles was determined using 1% agarose gel electrophoresis. To evaluate the release profiles of siRNA from PEI-Au/siRNA particles and PEI-Au/siRNA@ZGOC fibres, all the samples were treated with 4 mL of 2 % sodium dodecyl sulfate (SDS) and incubated for 20 min at room temperature. To evaluate the protection of siRNA by the two vectors, RNaseA (1 µL, 1 µg/µL) was used to digest siRNAs at 37 °C for 1 h, and EDTA (4 mL, 0.25 M) was used to inactivate RNaseA and incubated for 10 min at room temperature. Subsequently, 1% SDS solution (5 µL, 1 M) was added to dissociate siRNA from the two complexes.

Intracellular Trafficking of PEI-Au NRs/siRNA and PEI-Au/siRNA@ZGOC Systems

To monitor intracellular trafficking, PEI-Au/siRNA^{FAM} samples labeled with green fluorescence were incubated with HepG2 cells in 24-well plates (5×10^4 cells per well) at 37 °C for 18–20 h under 5% CO₂. The culture solution was discarded after the PEI-Au NRs/siRNA^{FAM} particles and PEI-Au/siRNA^{FAM}@ZGOC fibres were co-cultured with cells at different time points (2, 4, 6 and 8 h). Cells were fixed with 4 % paraformaldehyde and stained with LysoTracker Red (Invitrogen) and DAPI. Images were obtained using a Fluo View™ 1000 confocal microscope.

In vitro Anticancer Assay

HepG2 cells were used to examine the in vitro antitumor properties of PEI-Au/siRNA nanoparticles and PEI-Au/siRNA@ZGOC nanofibers. The cytotoxicity of the materials was examined using an MTT-based assay. Cells were seeded in 96-well culture plates (10^4 cells per well) in medium containing 10 % serum and allowed to adhere overnight at 37 °C under 5 % CO₂. Cells were then treated with the samples of various concentrations (0, 25, 50, 75 and 100 µg/mL) for 24, 48 and 72 h, respectively. At each time point, cell viability was determined, and the experiments were performed in triplicate on three separate occasions.

In vitro Gene Silencing Efficiency: qPCR analysis & Western blots

HepG2 cells were seeded in 6-well plates (2×10^5 cells per well) and incubated with PEI-Au/siRNA particles and PEI-Au/siRNA@ZGOC complexes (50 µg/mL) for 48 h and 72 h before qPCR analysis and Western blotting respectively. Total RNA was collected from transfected HepG2 cells using the EZ-10 Total RNA Mini-Preps Kits. 2 µg of extracted RNA was transcribed into cDNA using the First Strand cDNA Synthesis Kit according to the protocol provided. Subsequently, 2 mL of cDNA was subjected to qPCR analysis. The primer sequences for hTERT and GAPDH mRNA amplification are shown in Table 1. Proteins were extracted using a RIPA extraction reagent, separated on 8 % SDS-PAGE gel electrophoresis and transferred to a PVDF membrane (0.45 µm). Cells were co-cultured with the samples for 1 hour and irradiated with an LED lamp for 5 minutes every hour over the first 6 hours.

Conflicts of interest

There are no conflicts to declare.

Acknowledgements

This work was financially supported by the National Nature Science Foundation of China (51672247), the '111' Program funded by Education Ministry of China and State Administration of Foreign Experts Affairs (B16043), the Major State Research Program of China (2016YFC1101900).

References

- 1 K. V. Morris and D. J. Looney, *Science*, 2004, **305**, 1289–1292.
- 2 L. Aagaard and J. J. Rossi, *Adv. Drug Deliv. Rev.*, 2007, **59**, 75–86.
- 3 M. Nakamura, K. Masutomi, S. Kyo, M. Hashimoto, Y. Maida, T. Kanaya, M. Tanaka, W. C. Hahn and M. Inoue, *Human Gene Therapy*, 2005, **16**, 859–868.
- 4 L. Wang, J. Shi, H. Zhang, H. Li, Y. Gao and Z. Wang, *Biomaterials*, 2013, **34**, 262–274.
- 5 Y. Xie, H. Qiao, Z. Su, M. Chen, Q. Ping and M. Sun, *Biomaterials*, 2014, **35**, 7978–7991.
- 6 Y. Deng, C. C. Wang, K. W. Choy, Q. Du, J. Chen, Q. Wang, L. Li, T. K. Chung and T. Tang, *Gene*, 2014, **538**, 217–227.
- 7 S. J. Lee, M. J. Kim, I. C. Kwon and T. M. Roberts, *Adv Drug Deliv Rev*, 2016, **104**, 2–15.
- 8 R. Acharya, S. Saha, S. Ray, S. Hazra, M. K. Mitra and J. Chakraborty, *Materials science & engineering. C, Materials for biological applications*, 2017, **76**, 1378–1400.
- 9 H. J. Kim, A. Kim, K. Miyata and K. Kataoka, *Adv Drug Deliv Rev*, 2016, **104**, 61–77.
- 10 Y. Li, H. Wang, K. Wang, Q. Hu, Q. Yao, Y. Shen, G. Yu and G. Tang, *Small*, 2017, **13**, 1602697.
- 11 H. Kim and W. J. Kim, *Small*, 2014, **10**, 117–126.
- 12 C. Ma, L. Shi, Y. Huang, L. Shen, H. Peng, X. Zhu and G. Zhou, *Biomaterials science*, 2017, **5**, 494–501.
- 13 S. Rietwyk and D. Peer, *ACS nano*, 2017, **11**, 7572–7586.
- 14 M. W. Amjad, P. Kesharwani, M. C. I. Mohd Amin and A. K. Iyer, *Progress in Polymer Science*, 2017, **64**, 154–181.
- 15 J. Li, C. W. T. Leung, D. S. H. Wong, J. Xu, R. Li, Y. Zhao, C. Y. Y. Yung, E. Zhao, B. Z. Tang and L. Bian, *ACS applied materials & interfaces*, 2017, **xxx**, xxx–xxx.
- 16 D. Lee, K. Upadhye and P. N. Kumta, *Materials Science and Engineering: B*, 2012, **177**, 289–302.
- 17 C. Zhang, Y. Yong, L. Song, X. Dong, X. Zhang, X. Liu, Z. Gu, Y. Zhao and Z. Hu, *Advanced healthcare materials*, 2016, **5**, 2776–2787.
- 18 J. Shen, H. C. Kim, C. Mu, E. Gentile, J. Mai, J. Wolfram, L. N. Ji, M. Ferrari, Z. W. Mao and H. Shen, *Advanced healthcare materials*, 2014, **3**, 1629–1637.
- 19 Z. Yang, T. Liu, Y. Xie, Z. Sun, H. Liu, J. Lin, C. Liu, Z. W. Mao and S. Nie, *Acta biomaterialia*, 2015, **25**, 194–204.
- 20 J. H. Choi, H. J. Hwang, S. W. Shin, J. W. Choi, S. H. Um and B. K. Oh, *Nanoscale*, 2015, **7**, 9229–9237.
- 21 B. K. Wang, X. F. Yu, J. H. Wang, Z. B. Li, P. H. Li, H. Wang, L. Song, P. K. Chu and C. Li, *Biomaterials*, 2016, **78**, 27–39.
- 22 Z. Wang, S. Li, M. Zhang, Y. Ma, Y. Liu, W. Gao, J. Zhang and Y. Gu, *Advanced science*, 2017, **4**, 1600327.
- 23 J. B. Wolinsky, Y. L. Colson and M. W. Grinstaff, *Journal of Controlled Release*, 2012, **159**, 14–26.
- 24 A. J. Meinel, O. Germershaus, T. Luhmann, H. P. Merkle and L. Meinel, *European journal of pharmaceuticals and biopharmaceutics: official journal of Arbeitsgemeinschaft fur Pharmazeutische Verfahrenstechnik e.V.*, 2012, **81**, 1–13.
- 25 X. Hu, S. Liu, G. Zhou, Y. Huang, Z. Xie and X. Jing, *Journal of controlled release: official journal of the Controlled Release Society*, 2014, **185**, 12–21.
- 26 S. S. Liow, Q. Dou, D. Kai, A. A. Karim, K. Zhang, F. Xu and X. J. Loh, *ACS Biomaterials Science & Engineering*, 2016, **2**, 295–316.
- 27 B. P. Purcell, D. Lobb, M. B. Charati, S. M. Dorsey, R. J. Wade, K. N. Zellars, H. Doviak, S. Pettaway, C. B. Logdon, J. A. Shuman, P. D. Freels, J. H. Gorman, 3rd, R. C. Gorman, F. G. Spinale and J. A. Burdick, *Nature materials*, 2014, **13**, 653–661.
- 28 X. Xu, Z. Huang, Z. Huang, X. Zhang, S. He, X. Sun, Y. Shen, M. Yan and C. Zhao, *ACS applied materials & interfaces*, 2017, **9**, 20361–20375.
- 29 P. Rai, S. Mallidi, X. Zheng, R. Rahmanzadeh, Y. Mir, S. Elrington, A. Khurshid and T. Hasan, *Adv. Drug Deliv. Rev.*, 2010, **62**, 1094–1124.
- 30 H. J. Cho, M. Chung and M. S. Shim, *J. Ind. Eng. Chem.*, 2015, **31**, 15–25.

- 31 A. Bessiere, S. Jacquart, K. Priolkar, A. Lecointre, B. Viana and D. Gourier, *Optics express*, 2011, **19**, 10131-10137.
- 32 Z. Pan, Y. Y. Lu and F. Liu, *Nature materials*, 2011, **11**, 58-63.
- 33 T. Maldiney, A. Bessiere, J. Seguin, E. Teston, S. K. Sharma, B. Viana, A. J. Bos, P. Dorenbos, M. Bessodes, D. Gourier, D. Scherman and C. Richard, *Nature materials*, 2014, **13**, 418-426.
- 34 Z. Li, Y. Zhang, X. Wu, X. Wu, R. Maudgal, H. Zhang and G. Han, *Advanced science*, 2015, **2**, 150001.
- 35 Z. Li, Y. Zhang, X. Wu, L. Huang, D. Li, W. Fan and G. Han, *Journal of the American Chemical Society*, 2015, **137**, 5304-5307.
- 36 Z. Zhou, W. Zheng, J. Kong, Y. Liu, P. Huang, S. Zhou, Z. Chen, J. Shi and X. Chen, *Nanoscale*, 2017, **9**, 6846-6853.
- 37 W. Fan, N. Lu, C. Xu, Y. Liu, J. Lin, S. Wang, Z. Shen, Z. Yang, J. Qu, T. Wang, S. Chen, P. Huang and X. Chen, *ACS nano*, 2017, **11**, 5864-5872.
- 38 J. Shi, M. Sun, X. Sun and H. Zhang, *Journal of Materials Chemistry B*, 2016, **4**, 7845-7851.
- 39 B. Viana, S. K. Sharma, D. Gourier, T. Maldiney, E. Teston, D. Scherman and C. Richard, *Journal of Luminescence*, 2016, **170**, 879-887.
- 40 Y. Li, M. Gecevicius and J. Qiu, *Chemical Society reviews*, 2016, **45**, 2090-2136.
- 41 X. Ye, Linghua Jin, H. Caglayan, J. Chen, G. Xing, C. Zheng, V. Doan-Nguyen, N. E. Yijin Kang, C. R. Kagan and C. B. Murray, *ACS nano*, 2012, **6**, 2804-2817.
- 42 A. Zintchenko, A. Philipp, A. Dehshahri and E. Wagner, *Bioconjugate chemistry*, 2008, **19**, 1448-1455.
- 43 Z. Zhang, L. Wang, J. Wang, X. Jiang, X. Li, Z. Hu, Y. Ji, X. Wu and C. Chen, *Advanced materials*, 2012, **24**, 1418-1423.
- 44 Y. Fu, H. Liu, Z. Ren, X. Li, J. Huang, S. Best and G. Han, *Journal of Materials Chemistry B*, 2017, **5**, 5128-5136.
- 45 J. Kim, J. Kim, C. Jeong and W. J. Kim, *Adv Drug Deliv Rev*, 2016, **98**, 99-112.
- 46 J. R. Melamed, R. S. Edelstein and E. S. Day, *ACS nano*, 2015, **9**, 6-11.
- 47 G. F. Lemkine and B. A. Demeneix, *Curr. Opin. Mol. Ther.*, 2001, **3**, 178-182.
- 48 S. P. Sherlock, S. M. Tabakman, L. M. Xie and H. J. Dai, *ACS nano*, 2011, **5**, 1505-1512.
- 49 L. Z. Feng, X. Z. Yang, X. Z. Shi, X. F. Tan, R. Peng, J. Wang and Z. Liu, *Small*, 2013, **9**, 1989-1997.
- 50 W. Xia, P. Wang, C. Lin, Z. Li, X. Gao, G. Wang and X. Zhao, *Journal of controlled release: official journal of the Controlled Release Society*, 2012, **157**, 427-436.
- 51 X. D. Zhu, Y. Sun, D. Chen, J. F. Li, X. Dong, J. Wang, H. W. Chen, Y. Wang, F. L. Zhang, J. X. Dai, R. P. Pirraco, S. J. Guo, A. P. Marques, R. L. Reis and W. Li, *Journal of Controlled Release*, 2017, **254**, 107-118.
- 52 Y. Fu, X. Li, C. Sun, Z. Ren, W. Weng, C. Mao and G. Han, *ACS applied materials & interfaces*, 2015, **7**, 25514-25521.
- 53 Y. Li, Y. Fu, Z. Ren, X. Li, C. Mao and G. Han, *Journal of materials chemistry. B*, 2017, **5**, 7504-7511.
- 54 H. Liu, Y. Fu, Y. Li, Z. Ren, X. Li, G. Han and C. Mao, *Langmuir: the ACS journal of surfaces and colloids*, 2016, **32**, 9083-9090.
- 55 J. Perezjuste, I. Pastorizasantos, L. Lizmarzan and P. Mulvaney, *Coordination Chemistry Reviews*, 2005, **249**, 1870-1901.
- 56 M. Grzelczak, J. Perez-Juste, P. Mulvaney and L. M. Liz-Marzan, *Chemical Society reviews*, 2008, **37**, 1783-1791